## CHAPTER 27

## Numerical Modeling of Wave Deformation with a Current

## Susumu OHNAKA\*, Akira WATANABE\*\* and Masahiko ISOBE\*\*\*

#### ABSTRACT

A numerical computation method for a wave field coexisting with a current is presented to study wave-current interaction on a slowly varying bottom topography. Derivation is given for a new set of time-dependent mildslope equations extended to a wave and current coexisting field, which can deal with wave deformation due to combined refraction, diffraction, reflection and breaking as well as to wave-current interaction. Discussion is made on the numerical computation schemes, boundary conditions and breaking conditions. Some examples of the numerical computations are shown for wave and current coexisting fields.

### 1. INTRODUCTION

Many efforts have been devoted to the evaluation of wave deformation in the shallow water region with numerical models. The mild-slope equation has been presented and used by Berkhoff (1972) to study combined wave refraction and diffraction on a slowly varying bottom topography. Watanabe and Maruyama (1986) have proposed a time-dependent version of the mildslope equation, which can be more easily solved numerically and can deal with not only the combined refraction, diffraction and reflection but also wave breaking and decay in the surf zone.

In these equations, however, wave-current interaction is ignored. Coastal and nearshore currents such as rip current, longshore current and river discharge flow affect the wave deformation and therefore it is important to estimate the wave-current interaction in order to accurately predict the nearshore waves and currents and the resultant sediment transport.

<sup>\*</sup> Research Engineer, Technical Research Institute, Toa Corporation, 1-3, Anzen-cyo, Tsurumi-ku, Yokohama, 230 Japan

<sup>\*\*</sup> Professor, Department of Civil Engineering, Univ. of Tokyo, Hongo 7-3-1, Bunkyo-ku, Tokyo, 113 Japan

<sup>\*\*\*</sup> Associate Professor, ditto

For a wave field coexisting with a varying current, three kinds of wave equations and models have been proposed by Booij (1981), Liu (1983) and Kirby (1984), respectively. All these three models employ elliptic-type differential equations which are in general difficult to numerically solve. Hence these models are often approximated by parabolic equations, and then they are not applicable to the wave field including significant reflection due to structures.

In the present study, a new set of the time-dependent mild-slope equations extended to a wave and current coexisting field is derived and the numerical computation method is discussed. Some results of the computation are compared with analytical solutions and experimental results. The model is also applied to computing waves and currents under practical conditions including the presence of structures with consideration of the wave-current interaction.

### 2. DERIVATION OF GOVERNING EQUATIONS

The mild-slope equation presented by Berkhoff (1972) is the secondorder partial differential equation. On the other hand, the time-dependent mild-slope equations proposed by Watanabe and Maruyama (1986) consist of two first-order equations, which are obtained by separating the original mildslope equation in terms of the water surface elevation and the flow rate. They also include a term for the energy dissipation due to breaking. The numerical computation is conducted for every time-step, and it is easy to deal with boundary conditions in general and to calculate local wave direction needed for introducing partially reflective boundaries and for solving the dispersion relation in a wave and current coexisting field.

As mentioned before, three kinds of elliptic equations have been proposed for a wave and current coexisting field. Among them, the equation proposed by Kirby (1984), which exactly satisfies the conservation equation of wave action, is given by

$$\frac{\mathrm{D}^{2}\phi}{\mathrm{D}t^{2}} + (\nabla \cdot v) \frac{\mathrm{D}\phi}{\mathrm{D}t} - \nabla \cdot (\mathcal{C} \cdot \mathcal{C}_{g} \nabla \phi) + (o^{2} - k^{2} \mathcal{C} \cdot \mathcal{C}_{g}) \phi = 0$$
(1)

where  $D / Dt = \partial / \partial t + \mathcal{U} \cdot \nabla$ ,  $\nabla$  is the horizontal gradient operator,  $\phi$  the complex velocity potential at the mean water level,  $\mathcal{U}$  the steady current velocity vector,  $\sigma$  the intrinsic angular frequency, k the wave number vector, and  $\mathcal{C}$  and  $\mathcal{C}_g$  the phase and group velocity vectors calculated with  $\sigma$ , which is determined from

$$\omega = \sigma + \hbar \cdot U, \qquad \sigma^2 = gh \tanh hh \tag{2}$$

where  $\omega$  is the apparent angular frequency, h the water depth, and g the acceleration due to gravity. The velocity potential at an elevation z will be given by

$$\Phi(x, z, t) = \phi(x, t) f(z)$$
(3)

where f(z) is the vertical distribution function represented by

$$f(z) = \cosh k \left( h + z \right) / \cosh kh \tag{4}$$

Now we separate Eq. (1) into two equations expressed in terms of the surface elevation  $\zeta$  and the flow rate vector Q instead of  $\phi$ . The flow rate vector Q is defined by

$$Q = \int_{-h}^{0} \nabla \phi \, dz \tag{5}$$

Substituting Eqs. (3) and (4) into Eq. (5), we obtain

$$Q = C^2 \nabla \phi / g \tag{6}$$

On the other hand, the kinematic boundary condition at the water surface including the convection term due to a steady current requires

$$\zeta = -(1/g) \,\mathrm{D}\phi \,/\,\mathrm{D}t \tag{7}$$

Here the complex velocity potential  $\phi$  is expressed in terms of the amplitude and the phase as

$$\phi = \phi(\mathfrak{x}) e^{i\Psi} \tag{8}$$

where  $\Psi = \mathbf{k} \cdot \mathbf{x} - \omega t$  is the phase function. When we ignore change in the amplitude of the velocity potential as compared with change in the phase,  $D\phi/Dt$  is represented as

$$D\phi / Dt = -i\sigma\phi \tag{9}$$

Substitution of Eq. (9) into Eq. (7) yields the following expression of the surface elevation  $\zeta$  in terms of  $\phi$ :

$$\zeta = i(o/g)\phi \tag{10}$$

Substituting Eq. (10) into Eq. (5) and differentiating with t, we obtain

$$\partial Q/\partial t + \omega C^2 \nabla (\zeta/o) = 0 \tag{11}$$

On the other hand, using Eqs. (7) and (9),  $\phi$  is expressed as

$$\phi = (g/\sigma\omega) \,\partial\zeta/\partialt \tag{12}$$

Substituting Eqs. (6), (7) and (12) into Eq. (1), we obtain

$$m \,\partial\zeta/\partial t + \nabla \cdot (U\zeta) + \nabla \cdot (nQ) = 0, \tag{13}$$
$$m = 1 + (\sigma/\omega) (n-1), \qquad n = \mathbb{C}_{\sigma}/\mathbb{C}$$

Equations (11) and (13) are time-dependent mild-slope equations extended to a wave and current coexisting field. If we set the steady current velocity vector U = 0, these equations reduce to the ones proposed by Watanabe and Maruyama (1986), though the latter include an additional term for the energy dissipation due to breaking.

## 3. NUMERICAL COMPUTATION METHOD

Equations (11) and (13) are solved by using a finite difference method. A study area is divided into grid cells and a staggered mesh scheme is employed as shown in Fig. 1. Successive computation is conducted alternately for the flow rate Q and for the water surface elevation  $\zeta$ . If the convection term due to the steady current in Eq. (13) is neglected, Eqs. (11) and (13) can be easily solved by using an explicit finite difference scheme. However, when this terms is included as needed for general wave and current coexisting systems, some problems appear in numerical computations, such as numerical diffusion and unphysical reflection from the boundaries. In order to determine the most appropriate one among various finite difference schemes, we consider a one-dimensional wave and current field. The following notation is used.

$$\zeta_{i}^{j} = \zeta(i\Delta x, j\Delta x) \tag{14}$$

$$Q_{i}^{i} = Q\{(i+1/2)\Delta x, (j+1/2)\Delta t\}$$
(15)

namely the subscript i denotes the spatial point and the superscript j denotes the time-step. Equations (11) and (13) for the one-dimensional case are discretized to yield

$$m_{i} \frac{\zeta_{i}^{j+1} - \zeta_{i}^{j}}{\Delta t} + \frac{\delta(U\zeta)}{\delta x} + \frac{n_{i}Q_{i}}{\Delta x} - \frac{n_{i-1}Q_{i-1}}{\Delta x} = 0$$
(16)

$$\frac{Q_{i}^{j+1} - Q_{i}^{j}}{\Delta t} + \omega C_{i}^{2} \frac{(\zeta/\sigma)_{i+1}^{j} - (\zeta/\sigma)_{i}^{j}}{\Delta x} = 0$$
(17)

where  $m_i = 1 + (\sigma_i / \omega) (n_i - 1)$ . In Eq. (17), the flow rate  $Q_i^{j+i}$  can be calculated explicitly since the surface elevations  $\zeta_{i+1}^{j}$  and  $\zeta_i^{j}$  are known values. The problem is how to discretize the convection term  $\delta(U\zeta) / \delta x$  in Eq. (16).

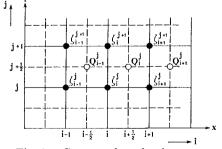


Fig. 1 Staggered mesh scheme.

<u> </u>	[]			
L	type		grid model	numerical diffusion term
implicit type	I	$\frac{1}{2}\left(\frac{\zeta_{1}^{+},\frac{1}{2},\frac{1}{2},\frac{1}{2},\frac{1}{2}}{\Delta_{1}}+\frac{\zeta_{1}^{+},\frac{1}{2},\frac{1}{2},\frac{1}{2}}{\Delta_{1}}\right)$ $U \ge 0$ $\frac{1}{2}\left(\frac{\zeta_{1}^{+},\frac{1}{2},\frac{1}{2},\frac{1}{2},\frac{1}{2}}{\Delta_{1}}+\frac{\zeta_{1}^{+},\frac{1}{2},\frac{1}{2},\frac{1}{2}}{\Delta_{1}}\right)$ $U < 0$	$\begin{array}{c} + & & & & \\ & & & & \\ & & & & \\ & & & &$	$-\frac{U}{2} \bigtriangleup x \frac{\partial^{2} \zeta}{\partial x^{2}}$
	п	$\frac{1}{2}\left(\frac{\zeta_{1+1}^{1+1}-\zeta_{1-1}^{1+1}}{2\bigtriangleup x}+\frac{\zeta_{1+1}^{1}-\zeta_{1-1}^{1}}{2\bigtriangleup x}\right)$		
explicit type	IJ	$\frac{\zeta_{1+1}^{2}-\zeta_{1}^{2}}{\Delta x} \qquad \qquad U \ge 0$	$ \begin{array}{c} \downarrow & \downarrow & \downarrow \\ \hline & \downarrow & \downarrow & \downarrow \\ \downarrow & \downarrow & \downarrow & \downarrow \\ j-1 & i & j+1 \end{array} $	$-\frac{U}{2}\Delta x \left(1-\frac{U\Delta t}{a\Delta x}\right) \frac{\partial^{3}\zeta}{\partial x^{2}} + \frac{U}{a}\Delta t$
		$\frac{\zeta'_{i}-\zeta'_{i-1}}{\Delta x} \qquad U < 0$	j+1 j+1 j-1 i i+1	$*\frac{\partial^{2}(nQx)}{\partial x^{2}} - \frac{\Delta t}{2} \frac{\partial^{2}(nQx)}{\partial x\partial t}$
	IV	$\frac{\zeta'_{1+1}-\zeta'_{1-1}}{2\bigtriangleup x}$	j+1 j+1 j-1 i+1	$\frac{\frac{U^2}{2a}\Delta t}{\frac{\partial}{\partial x^2}} \frac{\frac{\partial}{\partial x^2} + \frac{U}{2a}\Delta t}{\frac{\partial}{\partial x^2} - \frac{\Delta t}{2} \frac{\partial}{\partial x^2} (nQx)}$
	v	$\frac{\zeta_{\frac{1+1}{2}}^{\frac{1+1}{2}}-\zeta_{\frac{1+1}{2}}^{\frac{1+1}{2}}}{\Delta x}$ $\zeta_{\frac{1+1}{2}}^{\frac{1+1}{2}}(\zeta_{\frac{1+1}{2}}^{\frac{1+1}{2}}+\zeta_{\frac{1+1}{2}}^{\frac{1}{2}})/2$ $\zeta_{\frac{1+1}{2}}^{\frac{1+1}{2}}(\zeta_{\frac{1+1}{2}}^{\frac{1+1}{2}}+\zeta_{\frac{1+1}{2}}^{\frac{1}{2}})/2$	j+1 j+1 j-1 i+1	

Table 1 Difference schemes for the convection term.

First we use two types of the modified Euler method, which is of an implicit scheme. Type I in Table 1 is an up-wind difference scheme. With this scheme, however, a numerical diffusion term shown in Table 1 is added to Eq. (16). Such a diffusion term doesn't appear when a central difference scheme (Type II) is used. types I and II are of implicit type, and therefore it will be hard to extend them to computations of two-diimensional wave fields.

Next we discuss explicit difference scheme. Type III is an up-wind difference scheme and Type IV is a central difference scheme. With either of these schemes, however, a numerical diffusion term is added to Eq. (16) as shown in Table 1. This problem is solved by adopting the Alternating Direction Explicit (A. D. E.) method as presented as Type V in Table 1. In this scheme a value at a point (i-1) at a time-step (j) is replaced with the value calculated at the time-step (j+1) just before. By using this method, Eq. (16) can be solved explicitly without numerical diffusion.

Now the treatment of nonreflective boundary condition is discussed. For the equations proposed by Watanabe and Maruyama (1986), which include no convection term due to currents, the nonreflective boundary condition is given by the flow rate. Namely the flow rate at a point x on

the boundary at time  $t, Q'_x$ , is calculated by the flow rate at the inner point  $x - \Delta x$  at time  $t - \tau, Q_x^{t-\tau}$ . If this boundary condition given by the

flow rate is used in the calculation for a wave and current coexisting field, the surface elevation at the point  $x + \Delta x/2$  is needed in orer to evaluate the convection term in Eq. (16) with the scheme of Type V. This point is, however, located outside the calculation region, and therefore we must give the convection term along the boundary by backward difference scheme. Using this scheme, the second term in Eq. (16) is evaluated at the point  $x - \Delta x/2$ , whereas the third term is evaluated at the point x. The difference of the evaluation points causes unphysical reflection from the boundary.

In order to evaluate these terms at the same point, the calculation region is extended up to the point  $x + \Delta x/2$  and the boundary condition is given by the surface elevation  $\zeta$  instead of the flow rate Q, as shown in Fig. 2. The surface elevation at the point  $x + \Delta x/2$  on the boundary at time t is given by the one at the inner point  $x - \Delta x/2$ , at the time  $t - \tau$ , using a characteristic line C+U, as :

$$\zeta_{x+\Delta x/2}^{t} = \zeta_{x-\Delta x/2}^{t-\tau}$$
(18)

where  $\tau$  is defined by

$$\tau = \Delta x / (C + U) \tag{19}$$

By using this boundary condition, the surface elevation at the point  $x + \Delta x/2$  on the boundary is given independently of the difference scheme. Surface elevations at inner points are given by A. D. E. difference scheme, which can evaluate the second and third terms in Eq. (16) at the same point, and consequently we can avoid unphysical reflection.

For the two-dimensional case,  $\tau$  is calculated from the next equation instead of Eq. (19).

$$\tau = \Delta x \cos a_n / (C + U) \tag{20}$$

where  $a_n$  is the direction angle of the incident wave component measured from the normal line to the boundary.

By applying this procedure to a nonreflective boundary, the offshore open boundary condition is set in terms of the surface elevation as

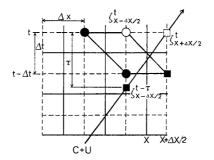


Fig. 2 Nonreflective boundary condition.

$$\zeta^{t}(x_{0}, y_{0}) = a_{i} \sin(hx_{0} + hy_{0} - \omega t) + \zeta^{t-\tau}_{R}(x_{0} + \Delta x, y_{0})$$

$$\zeta^{t-\tau}_{R}(x_{0} + \Delta x, y_{0}) = \zeta^{t-\tau}(x_{0} + \Delta x, y_{0})$$

$$- a_{i} \sin\{h(x_{0} + \Delta x) + hy_{0} - \omega t\}$$
(21)

where  $a_i$  is the incident wave amplitude.

### 4. RESULTS OF NUMERICAL COMPUTATION

To examine the applicability of these equations and method, numerical computations have been performed for two cases of wave deformation due to a current only.

The first case is a one-dimensional wave and current field as shown in Fig. 3. Figure 4 shows the wave height change in the shoreward direction in the steady state. In this figure H is the wave height, C the wave celerity and subscript  $_{o}$  denotes quantities at the location where no current exists. The wave heights change corresponding to the current intensity and direction. Waves freely pass through the nonreflective boundary, and no unphysical reflection appears.

Figure 5 shows time histories of the surface elevation at the boundary. The wave amplitudes and the arrival time to the boundary change according to the difference of currents.

The numerical computation results are compared with the analytical solutions in Fig. 6. Solid lines show the analytical solutions given by the wave action conservation equation, and solid circles show the numerical solutions. The numerical solutions agree quite well with the analytical solutions. On the other hand, if we neglect the scalar product  $k \cdot U$  in the dispersion relation, computations become easier particularly for a two-dimensional case. However if we set  $\sigma = \omega$ , both the numerical and analytical solutions deviate far from the true analytical solutions. From these results, it is confirmed that the scalar product  $k \cdot U$  in the dispersion relation cannot be neglected for a wave and current coexisting system.

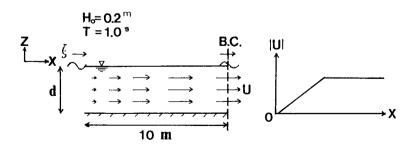


Fig. 3 Calculation condition for a one-dimensional wave and current field.

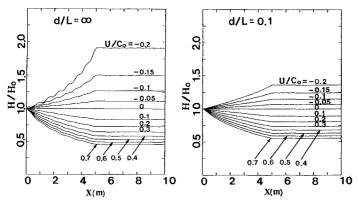


Fig. 4 Wave height change due to a current.

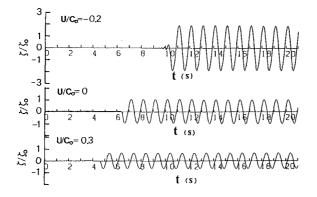


Fig. 5 Time history of the surface elevation at the boundary.

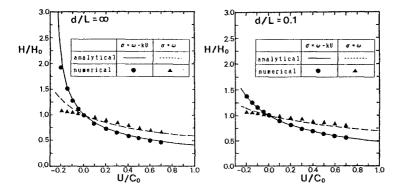


Fig. 6 Comparisons between numerical and analytical solutions of the wave height change due to a current.

The second case is for the wave refraction due to a current. The steady current is assumed to change in the x-direction only and waves are incident obliquely into the constant depth region as shown in Fig. 7. In this calculation, for the wave direction needed for solving the dispersion relation, the analytical solution given by Longuet-Higgins (1961) is adopted. The numerical solutions for the wave height and direction are compared with the analytical solutions in Fig. 8. Here the wave direction in the numerical calculation has been obtained from the principal direction of the flow rate vector. The numerical results agree well with the analytical solutions.

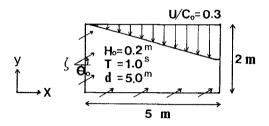


Fig. 7 Calculation condition for wave refraction due to a current.

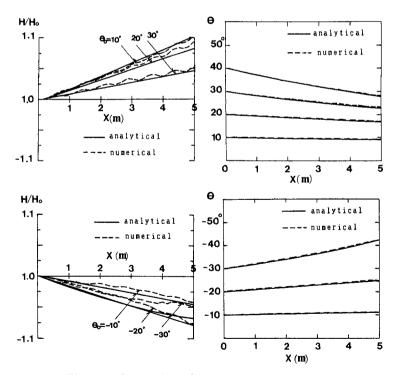


Fig. 8 Comparisons between numerical and analytical solutions of the wave height and direction.

# 5. DETERMINATION OF THE BREAKER LINE AND WAVES IN THE SURF ZONE

First we discuss the determination of the location of the breaker line which is very important to properly predict nearshore wave and current fields.

Goda (1970) has presented a breaker index diagram which is expressed in terms of the ratio of the depth at the breaking point  $h_b$  to the equivalent deepwater wave height  $H_o$ ' as a function of the deepwater wave steepness  $H_o'/L_o$  and the bottom slope s. This diagram can be used to evaluate the location of the breaking point of a single wave train. On the other hand, Watanabe *et al.* (1984) have proposed another breaker index diagram using the ratio of the amplitude of horizontal water particle velocity to the wave celerity at the breaking point,  $u_b / C_b$ , in order to extend to a composite wave field. This can be obtained from the Goda's breaker index diagram by converting the governing parameter from  $h_b / H_o$ ' to  $u_b / C_b$  with a linear wave theory. It will be applicable even to a wave and current coexisting system when a moving coordinate relative to the current is adopted.

In order to examine the applicability of this breaker index, a series of laboratory experiments have been carried out on the breaking of waves on a current with the same or the adverse direction. Using the breaking depth  $h_b$  obtained from the experimental results, the horizontal water particle velocity amplitude  $u_b$  at the mean water level and the wave celerity  $C_b$  are calculated with a linear wave theory as

$$u_b = (H_b/2) \sigma \cosh kh_b / \sinh kh_b \tag{22}$$

$$C_b = \sigma / k \tag{23}$$

where the wave number k and the angular frequency o are calculated from the dispersion relation for a wave and current coexisting system as the values relative to the current. The breaker height  $H_b$  is calculated from the incident wave height  $H_i$  considering the bottom and side wall friction as

$$E_i (C_i + U_i) / \sigma_i = E_b (C_b + U_b) / \sigma_b - \Delta E / \omega$$

$$E = (1/8) \rho g H^2$$
(24)

where U is the mean velocity of the current, subscripts *i* and *b* denote quantities at the locations where the incident wave height and the breaking point are respectively given, and  $\Delta E$  denotes the energy dissipation rate due to the bottom and side wall friction, which is calculated with the friction law from a wave and current coexisting system presented by Tanaka and Shuto (1981).

Using Eqs. (22) and (23), the ratio of the horizontal water particle

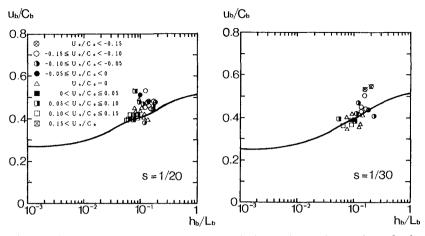


Fig. 9 Comparisons between the breaker index and experimental results for wave and current coexisting fields.

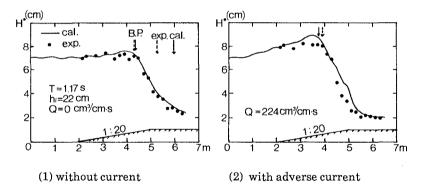
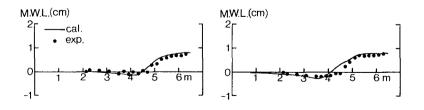


Fig. 10 Cross-shore distributions of the wave height.



(1) without current

(2) with adverse current

Fig. 11 Cross-shore distributions of the mean water level.

velocity to the wave celerity,  $u_b / C_b$ , is calculated. The relation between this ratio and the relative water depth at the breaking point,  $h_b / L_b$ , is compared with the breaker index proposed by Watanabe *et al.* (1984) in Fig. 9, where the bottom slope *s* is 1/20 and 1/30, respectively. Different symbols are used for the experimental results according to the ratio of the steady current velocity at the breaking point to the wave celerity at the deepwater. For the cases of a strong adverse direction current, the experimental results show larger values of  $u_b / C_b$  than the breaker index. This will be attributed to the acceleration of breaking, which is ignored in Eq. (24), due to the turbulence transported toward the offshore by the current. As a whole, the experimental results agree fairly well with the breaker index. Hence this breaker index is applicable with a sufficient accuracy to a wave and current coexisting field.

Using the time-dependent mild-slope equations proposed in this study together with the above breaker index, numerical computations have been conducted for the location of the breaking point and the deformation of waves coexisting with a current on a uniformly sloping beach. For the computation of wave decay in the surf zone, the dissipation term proposed by Watanabe *et al.* (1988) has been added to Eq. (11).

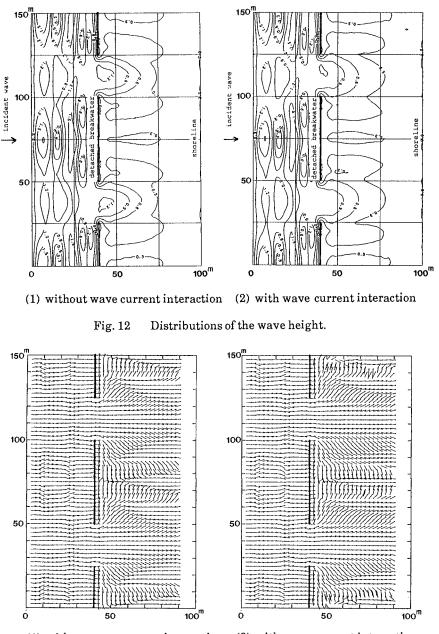
Figure 10 shows the comparisons of the computed and the experimental result of the wave height distributions. The left figure is for a case of no current, while the right figure is for an adverse current with the flow rate of 224 cm<sup>3</sup>/cm/s. The experimental values are represented by the wave heights calculated from the root mean square of the measured surface elevation as  $H^* = 2\sqrt{2} \eta_{rms}$ . The computed and the measured locations of the breaking point (B.P.) shows a good agreement regardless of the presence of currents. The wave height distributions also show a good overall agreement between the computations and the model. A slight overestimation of the wave height for the case of an adverse current is caused owing to the ignorance of the turbulence transported into the offshore across the breaking point by the current.

The comparisons of the mean water level between the computations and the measurements are shown in Fig. 11. The computed values agree well with the experimental results.

# 6. EXAMPLES OF THE NUMERICAL COMPUTATION FOR A PLANAR TWO-DIMENSIONAL CASE

The present numerical model has been applied to computing a wave field around detached breakwaters on a sloping beach. The detached breakwaters are placed at a water depth of 3 m and the bottom slope is 1/20. Waves are incident normal to the detached breakwaters and the contour lines, and the incident wave height and period are 3.0 m and 5.7 s.

In this computation including wave decay due to breaking, the wave height should become 0 along the shoreline, and therefore the shoreline boundary condition is set as



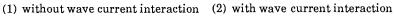
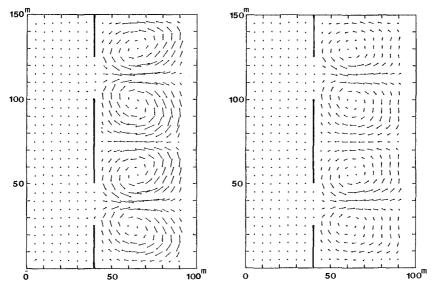


Fig. 13 Distributions of the wave direction.



(1) without wave current interaction (2) with wave current interaction

Fig. 14 Distributions of nearshore currents.

$$\zeta'(x_0, y_0) = 0 \tag{25}$$

Along the side boundaries, perfect reflection of waves and no-slip of mean currents are assumed.

Figure 12 shows distributions of the wave height with and without wave-current interaction : the figure on the left hand-side is the result without wave-current that with wave-current interaction. The change of the wave height can be observed when wave-current interaction is taken into consideration.

Distributions of the wave direction for both cases are shown in Fig. 13. Refraction due to the nearshore current is well observed near the shoreline.

Figure 14 show distributions of the nearshore current for both cases. Reduction of current can be observed when wave-current interaction is included.

# 7. CONCLUSIONS

A new set of time-dependent mild-slope equations has been derived for a wave and current coexisting field, and numerical computational method has been presented. Validity of this model has been demonstrated by comparisons of numerical results with analytical and experimental results. Then it has been found that the breaker index expressed by the ratio of the water particle velocity to the wave celerity is applicable to a wave and current coexisting system. Finally this model has been applied to general two-dimensional wave and current fields and it has been found that wave-current interaction plays an important role in nearshore waves and currents.

#### REFERENCES

- 1) Berkhoff, J.C.W. (1972) : Computation of combined refractiondiffraction, Proc. 13th Coastal Eng. Conf., ASCE, pp. 471-490.
- 2) Booij, N. (1981): Gravity waves on water with non-uniform depth and current, Communications on Hydraulics, No. 81-1, Dept. of Civil Eng., Delft Univ. of Tech., p. 131
- 3) Goda, Y. (1970): A synthesis of breaker indices, Proc. of the Japan Society of Civil Eng., No. 180, pp. 39-49.
- 4) Kirby, J. T. (1984) : A note on linear surface wave-current interaction over slowly varying topography, J. Geophys. Res., Vol. 89, No. C1, pp. 745-747.
- 5) Liu, P. L. F. (1983) : Wave-current interactions on slowly varying topography, J. Geophys. Res., Vol. 88, No. C7, pp.4421-4426.
- 6) Longuet-Higgins, M. S. and R. W. Steward (1961): The changes in amplitude of short gravity waves on steady non-uniform currents, J. fluid Mech., Vol. 10, pp. 529-549.
- 7) Tanaka, M. and N. Shuto (1981): Friction coefficient for a wave-current coexistent system. Coastal Eng. in Japan, Vol. 24, pp. 105-128.
- Watanabe, A., T. Hara and K. Horikawa (1984): Study on breaking condition for compound wave trains, Coastal Eng. in Japan, Vol. 27, pp.71-82.
- 9) Watanabe, A. and K. Maruyama (1986) : Numerical modeling of nearshore wave field under combined refraction, diffraction and breaking, Coastal Eng. in Japan, Vol. 29, pp. 19-39.
- 10) Watanabe, A. and M. Dibajnia (1988) : A numerical model of wave deformation in surf zone, Proc. 21st Coastal Eng. Conf., ASCE, (in print)